

# Supplementary Material for “Wilson–Fisher Renormalization of Discrete Surface-Wave Turbulence”

José A. Santiago, Mikheil Kharbedia, Basilio J. García, and Francisco Monroy  
(Dated: January 15, 2026)

This Supplementary Material provides the scaling arguments and renormalization-group (RG) considerations underlying the main text. In particular, we justify the definition of the running coupling, the Wilson–Fisher beta function, the topology-dependent nonlinear transfer rate, and we provide additional steps supporting the Reynolds-number scaling of the integrated inertial spectral weight reported in the main text.

## RUNNING COUPLING AND INERTIAL SPECTRA

We analyze the surface-velocity signal  $v(t)$  measured by laser Doppler vibrometry through its power spectral density  $S(\omega)$ , defined by  $\langle v^2 \rangle = \int_0^\infty S(\omega) d\omega$ . In the inertial interval, weak wave turbulence predicts Kolmogorov–Zakharov (KZ) power laws  $S(\omega) \sim \omega^{-p}$ , with  $p = 17/6$  for capillary waves and  $p = 5/2$  for gravity waves [1, 2].

At scaling level, the velocity variance carried by a logarithmic band around  $\omega$  is  $v_\omega^2 \sim S(\omega) \Delta\omega$  with  $\Delta\omega \sim \omega$ , hence

$$v_\omega^2 \sim \omega S(\omega). \quad (\text{S1})$$

Using  $v_\omega \sim \omega a_\omega$  to relate velocity to surface-displacement amplitude  $a_\omega$  then gives

$$a_\omega^2 \sim \frac{S(\omega)}{\omega}. \quad (\text{S2})$$

## DIMENSIONLESS NONLINEARITY AND RG COUPLING

For weakly nonlinear surface waves, the standard control of nonlinearity is the wave steepness  $\epsilon(\omega) \sim k(\omega)a_\omega$ , which measures the relative slope of the interface and sets the size of nonlinear frequency shifts and resonance broadening; accordingly, it is the small parameter underlying weak-turbulence closures [1, 2, 4]. Combining with Eq. (S2) yields

$$\epsilon(\omega)^2 \sim k(\omega)^2 \frac{S(\omega)}{\omega}. \quad (\text{S3})$$

This motivates the RG running coupling used throughout the main text,

$$g(\omega) \equiv \epsilon(\omega)^2, \quad (\text{S4})$$

which is dimensionless, scale dependent, and small in the DSWT regime.

## WILSON–FISHER BETA FUNCTION

Introducing the RG “time”  $\ell = \ln(\omega/\omega_0)$ , the inertial KZ-scaling and the dispersion relation  $k(\omega) \sim \omega^\alpha$  imply

$$g(\omega) \sim \omega^{y_g}, \quad y_g = 2\alpha - (p + 1), \quad (\text{S5})$$

where we used  $g(\omega) = \epsilon(\omega)^2 \sim k(\omega)^2 S(\omega)/\omega$  [Eq. (S3)] and  $S(\omega) \sim \omega^{-p}$ . At scaling level, the RG flow of the coupling may be written in Wilson–Fisher form,

$$\beta(g) \equiv \frac{dg}{d\ell} = y_g g - B_N g^{N-1}, \quad (\text{S6})$$

where  $N$  is the order of the resonant interaction ( $N = 3$  for capillary-wave triads and  $N = 4$  for gravity-wave tetrads), and  $B_N > 0$  encodes nonlinear saturation. Besides the unstable Gaussian fixed point  $g^* = 0$ , Eq. (S6) admits a nontrivial stable fixed point corresponding to the KZ inertial state discussed in the main text.

## TOPOLOGY-DEPENDENT NONLINEAR TRANSFER RATE

In wave turbulence theory, spectral transfer is mediated by resonant  $N$ -wave interactions. The interaction vertex is of order  $(N - 2)$  in the wave amplitude, and the collision integral governing spectral evolution is quadratic in this vertex. As a result, the nonlinear transfer rate scales as

$$\tau_{\text{nl}}^{-1}(\omega) \sim \omega \epsilon(\omega)^{2(N-2)}. \quad (\text{S7})$$

Substituting  $\epsilon(\omega)^2 \sim k(\omega)^2 S(\omega)/\omega$  [Eq. (S3)] into Eq. (S7) yields

$$\tau_{\text{nl}}^{-1}(\omega) \sim \omega \left[ \frac{k(\omega)^2}{\omega} S(\omega) \right]^{N-2}, \quad (\text{S8})$$

which reproduces the bridge relation used in the main text in velocity-PSD form and makes explicit that the dependence on interaction topology enters solely through the exponent  $N - 2$ .

## MATCHING TO VISCOUS DISSIPATION: KOLMOGOROV CUTOFF SCALING (SUPPORT FOR FIGURE 2)

Viscous damping originates from the Navier–Stokes operator  $\nu \nabla^2 \mathbf{u}$  and yields, at scaling level, a universal dissipation rate

$$\tau_\nu^{-1}(k) \sim \nu k^2. \quad (\text{S9})$$

The ultraviolet cutoff frequency is experimentally identified as the Kolmogorov cutoff  $\omega_K$  (Fig. 1 of the main text) and its renormalized scaling with forcing is reported in Fig. 2. It is selected by the crossover condition

$$\tau_{\text{nl}}(\omega_K) \sim \tau_\nu(\omega_K), \quad (\text{S10})$$

which terminates the RG flow at finite scale.

To compare different fluids and dispersive regimes, we normalize the exit frequency by the viscous decay rate of the *injection* mode. Let  $k_0 \equiv k(\omega_0)$  be the driven wavenumber selected by the dispersion relation at the fixed forcing frequency  $\omega_0$ . We define the dimensionless ultraviolet coordinate

$$\bar{\Omega}_\nu \equiv \frac{\omega_K}{\nu k_0^2} = \frac{\text{exit rate}}{\text{viscous decay rate at injection}}, \quad (\text{S11})$$

which measures how far the cascade extends before being arrested by viscous dissipation, in units of the injection-scale viscous rate  $\tau_\nu^{-1}(k_0) \sim \nu k_0^2$ . This normalization does not require  $k_0$  to be invariant across fluids; it relies only on the microscopic Navier–Stokes operator evaluated at the forced mode.

The definition (S11) cleanly separates the RG-generated ultraviolet extent of the cascade, set by the balance (S10) at the exit scale, from the bare dissipative rate fixed at injection. Changing the precise numerical definition of  $k_0$  by an  $\mathcal{O}(1)$  factor rescales  $\bar{\Omega}_\nu$  by a constant prefactor but leaves the measured power-law exponents unchanged. The observed Wegner-like crossover scaling in Fig. 2 therefore reflects a genuine Wilsonian property of the viscous cutoff, not an artifact of a particular injection-scale convention. Using the topology-dependent transfer rate in velocity-PSD form,

$$\tau_{\text{nl}}^{-1}(\omega) \sim \omega \left[ \frac{k(\omega)^2}{\omega} S(\omega) \right]^{N-2}, \quad (\text{S12})$$

(see Eq. (S8)), the cutoff inherits its forcing dependence through the inertial KZ spectrum  $S(\omega) \sim \Pi^\chi \omega^{-p}$ , where  $\Pi$  is the conserved energy flux and  $\chi$  is fixed by weak-turbulence theory [1, 2]. At fixed driving frequency  $\omega_0$ , the injected kinetic-energy density  $E = \frac{1}{2} \rho U_0^2$  sets the flux at scaling level,  $\Pi \propto E$  (up to  $\omega_0$ -dependent constants). Combining these scalings with  $k(\omega) \sim \omega^\alpha$  in the matching condition (S10) yields the topology-dependent cutoff laws reported in the main text and validated by the collapse in Fig. 2,

$$\bar{\Omega}_\nu^{(C)} \sim \bar{E}^{2/3} \quad (N = 3), \quad \bar{\Omega}_\nu^{(G)} \sim \bar{E}^1 \quad (N = 4). \quad (\text{S13})$$

For each forcing series performed at fixed  $\omega_0$ , the ultraviolet reach may equivalently be parametrized by  $\bar{\Omega}_\omega \equiv \omega_K/\omega_0$ ; however,  $\bar{\Omega}_\nu$  is the more universal normalization across fluids, as it explicitly removes the fluid-dependent viscous rate at injection. In this sense,  $\bar{\Omega}_\nu$  is a genuinely Wilsonian ultraviolet coordinate: it compares the RG-generated exit scale  $\omega_K$  to the bare dissipative operator inherited from microscopic hydrodynamics. The reduced forcing is expressed as  $\bar{E} \equiv E/E_0$ , with  $U_0 = A\omega_0$  and viscous reference energy

$$E_0 \equiv \rho \left( \frac{\nu}{\Lambda_0} \right)^2, \quad \Lambda_0 \equiv \frac{2\pi}{k_0}. \quad (\text{S14})$$

Here  $\Lambda_0$  is the injection wavelength selected by the linear dispersion relation at  $\omega_0$ . Physically,  $E_0$  is the kinetic-energy density associated with viscous relaxation over one forcing wavelength, so that  $\bar{E} \sim (U_0\Lambda_0/\nu)^2$  measures the distance from the viscous (Gaussian) regime using only injection-scale quantities, isolating the topology-controlled renormalization of the ultraviolet cutoff.

### INTEGRATED INERTIAL SPECTRAL WEIGHT: REYNOLDS SCALING (SUPPORT FOR FIGURE 3)

We connect the experimentally accessible integrated inertial spectral weight

$$\Sigma_{\text{PSD}} \equiv \int_{\omega_0}^{\omega_K} S(\omega) d\omega, \quad (\text{S15})$$

to the Reynolds-number scaling reported in Fig. 3 of the main text. Here  $S(\omega)$  is the surface-velocity PSD measured by LDV, so  $\Sigma_{\text{PSD}}$  has units of velocity squared and represents the total velocity variance accumulated in the direct cascade between the pump and the ultraviolet exit scale. The upper limit  $\omega_K$  is retained because it marks the experimentally resolved exit from the inertial basin; however, for the steep inertial spectra observed here ( $p > 1$ ), extending the integral to  $\infty$  does not affect scaling exponents (the integral is pump-dominated).

#### 1. Pump-dominated integral and flux prefactor

For a stationary direct energy-flux cascade, the inertial KZ spectrum takes the scaling form

$$S(\omega) \sim C_N \Pi^\xi \omega^{-p}, \quad (\text{S16})$$

where  $\Pi$  is the constant energy flux through the inertial interval and  $\xi$  is fixed by weak-turbulence scaling for the relevant  $N$ -wave kinetic equation [1, 2]. Substituting Eq. (S16) into Eq. (S15) gives, for  $p \neq 1$ ,

$$\Sigma_{\text{PSD}} \sim \Pi^\xi \frac{\omega_K^{1-p} - \omega_0^{1-p}}{1-p}. \quad (\text{S17})$$

Because  $p > 1$  in both classes, the integral is dominated by its lower limit, so at scaling level

$$\Sigma_{\text{PSD}} \sim \Pi^\xi \omega_0^{1-p} \quad (p > 1), \quad (\text{S18})$$

with  $\omega_K$  contributing only a subleading correction  $\propto \Pi^\xi \omega_K^{1-p}$ .

#### 2. Reduced response coordinate and Reynolds control

We define as reduced (dimensionless) cascade response the forcing-normalized integrated variance

$$\bar{\Sigma}_\omega \equiv \frac{\Sigma_{\text{PSD}}}{(\Lambda_0\omega_0)^2} = \frac{\text{inertial velocity variance above the pump}}{\text{forcing-scale velocity squared}}, \quad \Lambda_0 \equiv \frac{2\pi}{k_0}, \quad (\text{S19})$$

where  $k_0$  is the driven wavenumber selected by the dispersion relation at the fixed forcing frequency  $\omega_0$ . This is the appropriate response coordinate for Fig. 3 because it removes only the trivial forcing-scale units and leaves viscosity to enter solely through renormalization. A viscous normalization,  $\Sigma_{\text{PSD}}/(\nu/\Lambda_0)^2$ , would divide by the relevant perturbation itself and hard-wire an explicit  $\nu^{-2}$  factor, masking the crossover physics.

In the pump-dominated regime  $p > 1$ , Eqs. (S18)–(S19) imply, at fixed  $\omega_0$  and  $\Lambda_0$ ,

$$\bar{\Sigma}_\omega \sim \Pi^\xi, \quad (\text{S20})$$

so the Reynolds dependence of  $\bar{\Sigma}_\omega$  reflects how viscosity renormalizes the inertial flux (equivalently the injection-scale coupling).

The experimentally accessible control parameter is the injection Reynolds number

$$\text{Re} = \frac{U_0 \Lambda_0}{\nu}, \quad U_0 = A \omega_0. \quad (\text{S21})$$

### 3. WF/Wegner scaling and quadratic response to the WF field

The Wilson–Fisher (WF) framework promotes the squared steepness  $g(\omega) = \epsilon(\omega)^2$  to a running coupling whose flow is controlled by

$$\beta(g) = \frac{dg}{d\ell} = y_g g - B_N g^{N-1}, \quad \ell \equiv \ln(\omega/\omega_0), \quad (\text{S22})$$

with interaction topology fixing the first nonlinear saturation channel  $g^{N-1}$  (triads:  $N = 3$  for CW; tetrads:  $N = 4$  for GW). The reduced response follows a Wegner crossover form,

$$\bar{\Sigma}_\omega(\text{Re}) = \text{Re}^{\kappa_N} \mathcal{F}_N \left( \frac{\text{Re}}{\text{Re}_\times} \right), \quad (\text{S23})$$

where  $\mathcal{F}_N$  is topology dependent and  $\text{Re}_\times$  is nonuniversal. The key closure supported by Fig. 3 is that the forcing-normalized integrated variance is quadratic in the coarse-grained WF field at injection,

$$\bar{\Sigma}_\omega \propto g_0^2, \quad g_0 \equiv g(\omega_0). \quad (\text{S24})$$

This dependence is dynamical: in weak WT the transfer amplitude is proportional to the interaction vertex and hence to the steepness  $\epsilon$ , so the leading variance production above the pump scales as the square of that amplitude,  $\sim \epsilon^2$ . Since  $g = \epsilon^2$ , the leading cascade-induced contribution scales as  $\delta\bar{\Sigma}_\omega \sim g_0^2$ , consistent with the lowest non-vanishing self-renormalizations summarized in End Matter, Fig. 4.

### 4. Topology-controlled Reynolds scaling of the cascade response

In the asymptotic WF regime ( $\text{Re} \gg \text{Re}_\times$ ), the crossover function in Eq. (S23) saturates, so  $\bar{\Sigma}_\omega \sim \text{Re}^{\kappa_N}$ . To determine  $\kappa_N$ , we write the injection-scale effective coupling as the single-parameter crossover ansatz  $g_0 \sim \text{Re}^{\gamma_N}$ . The exponent  $\gamma_N$  is fixed by topology: the first nonlinear feedback that arrests the WF growth is the  $g^{N-1}$  term in Eq. (S22), so the minimal injection-level equation of state is  $\text{Re} \propto g_0^{N-1}$ , i.e.

$$g_0 \sim \text{Re}^{1/(N-1)}. \quad (\text{S25})$$

Combining Eq. (S25) with the quadratic response law Eq. (S24) gives

$$\bar{\Sigma}_\omega \sim \text{Re}^{2/(N-1)}, \quad (\text{S26})$$

hence  $\kappa_N = 2/(N-1)$ . Therefore,

$$\bar{\Sigma}_\omega^{(CW)} \sim \text{Re}^1 \quad (N=3), \quad \bar{\Sigma}_\omega^{(GW)} \sim \text{Re}^{2/3} \quad (N=4), \quad (\text{S27})$$

in agreement with the collapse in Fig. 3 of the main text.

## RAW INTEGRATED INERTIAL SPECTRAL WEIGHT (SUPPLEMENTARY FIG. S1)

We report the non-normalized integrated inertial spectral weight

$$\Sigma_{\text{PSD}} \equiv \int_{\omega_0}^{\omega_K} S(\omega) d\omega, \quad (\text{S28})$$

where  $S(\omega)$  is the LDV surface-velocity PSD and  $\omega_K$  is the experimentally resolved viscous cutoff. Since  $\Sigma_{\text{PSD}}$  has units of velocity squared, it measures the total velocity variance accumulated in the direct cascade between the pump and the ultraviolet exit scale.

Supplementary Fig. S1 plots  $\Sigma_{\text{PSD}}$  versus the forcing velocity  $U_0 = A\omega_0$  for gravity-wave (GW) and capillary-wave (CW) cascades across all fluids. In both classes,  $\Sigma_{\text{PSD}}$  increases monotonically with forcing, showing direct activation of the inertial response above the pump. The raw curves are not expected to collapse because  $\Sigma_{\text{PSD}}$  retains explicit dependence on the forcing scale and material parameters; the corresponding reduced response  $\bar{\Sigma}_\omega$  and its Reynolds renormalization are reported in Fig. 3 of the main text.

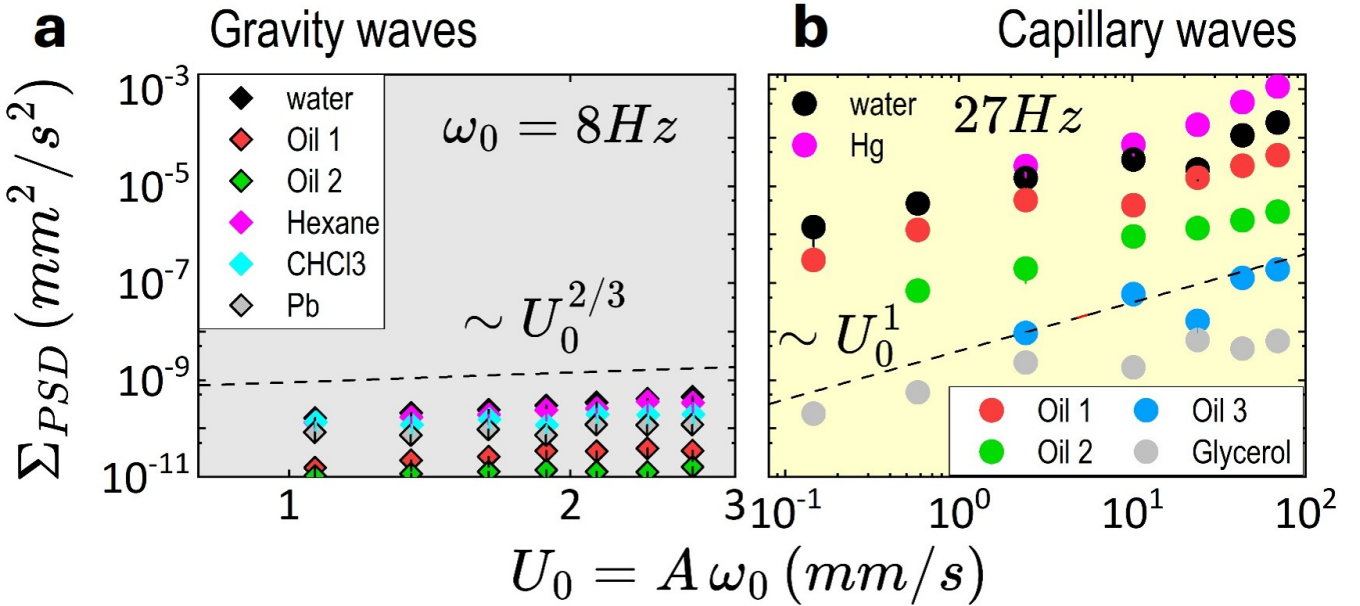


**FIG. 1. Supplementary Fig. S1: Raw integrated inertial spectral weight.** Integrated inertial spectral weight  $\Sigma_{\text{PSD}} = \int_{\omega_0}^{\omega_K} S(\omega) d\omega$  (LDV surface-velocity PSD) versus forcing velocity  $U_0 = A\omega_0$  for gravity waves (left;  $\omega_0 = 8 \text{ Hz}$ ) and capillary waves (right;  $\omega_0 = 27 \text{ Hz}$ ), across all fluids (legend). The GW branch lies  $\sim 3$  decades below the CW branch over the full forcing range. The forcing-normalized response  $\bar{\Sigma}_\omega \equiv \Sigma_{\text{PSD}}/(\Lambda_0\omega_0)^2$  and its Reynolds renormalization are shown in Fig. 3 of the main text.

## ORTHOGONALITY OF RG COORDINATES: EXIT SCALE VERSUS RESPONSE

The two reduced observables used in the main text, the exit coordinate  $\bar{\Omega}_\nu$  (Fig. 2) and the cascade response  $\bar{\Sigma}_\omega$  (Fig. 3), probe complementary pieces of the WF structure. The exit coordinate  $\bar{\Omega}_\nu = \omega_K/(\nu k_0^2)$  is normalized by the viscous decay rate of the injection mode, so it measures the ultraviolet reach of the inertial basin relative to the bare Navier-Stokes dissipative operator. By contrast,  $\bar{\Sigma}_\omega = \Sigma_{\text{PSD}}/(\Lambda_0\omega_0)^2$  is normalized only by forcing-scale quantities and measures the strength of the cascade, i.e. the velocity variance accumulated above the pump; using a viscous normalization here would mix the response with the relevant perturbation that drives the crossover. This asymmetric normalization is deliberate:  $\bar{\Omega}_\nu$  quantifies where the flow stops (viscous arrest), whereas  $\bar{\Sigma}_\omega$  quantifies how strongly it proceeds (nonlinear saturation). Together,  $(\bar{\Omega}_\nu, \bar{\Sigma}_\omega)$  form an orthogonal pair of RG coordinates that separately resolve reach and intensity in DSWT.

## SCOPE OF VALIDITY

The arguments presented here are valid at the scaling level within the weakly nonlinear DSWT regime, where (i) the inertial interval exhibits KZ-type power-law behavior, (ii) transfer is mediated predominantly by the resonant interaction topology ( $N = 3$  for CW and effective  $N = 4$  for GW), and (iii) viscous damping can be represented at scaling level by  $\tau_\nu^{-1}(k) \sim \nu k^2$ . The crossover matching  $\tau_{\text{nl}}(\omega_K) \sim \tau_\nu(\omega_K)$  is intended as a scaling criterion for the exit from the inertial basin.

### Weak-nonlinearity diagnostic

We monitored the forcing-scale steepness  $\epsilon_0 \equiv k_0 A$  as a dimensionless proxy for nonlinear frequency shifts and resonance broadening. Across all datasets reported here,  $\epsilon_0$  remains in the range

$$10^{-3} \lesssim \epsilon_0 \lesssim 10^{-1},$$

well below unity and firmly within the weakly nonlinear regime. In this range, the pump remains spectrally sharp, higher harmonics are subdominant, and a clear KZ-type inertial interval is resolved above  $\omega_0$ .

As  $\epsilon_0$  approaches unity, nonlinear frequency shifts become comparable to linear mode spacing, leading to strong resonance broadening, cluster overlap, and eventual breakdown of topology-controlled transfer. Such conditions are expected to invalidate the present Wilson–Fisher crossover description and drive a transition toward strong (Philips-like) turbulence, a regime not explored in the present experiments.

- [1] V. E. Zakharov, V. S. L'vov, and G. Falkovich, *Kolmogorov Spectra of Turbulence I: Wave Turbulence* (Springer, Berlin, 1992).
- [2] S. Nazarenko, *Wave Turbulence* (Springer, Heidelberg, 2011).
- [3] V. E. Zakharov and N. N. Filonenko, Sov. Phys. JETP **24**, 377 (1967) [Zh. Eksp. Teor. Fiz. **51**, 588 (1966)].
- [4] F. Dias and C. Kharif, Annu. Rev. Fluid Mech. **31**, 301 (1999).
- [5] A. I. Dyachenko, A. C. Newell, A. N. Pushkarev, and V. E. Zakharov, Phys. Rev. Lett. **92**, 134501 (2004).
- [6] E. Kartashova, Phys. Rev. Lett. **98**, 214502 (2007).
- [7] E. Kartashova, Europhys. Lett. **87**, 44001 (2009).
- [8] F. J. Wegner, Phys. Rev. B **5**, 4529 (1972).
- [9] L. D. Landau and E. M. Lifshitz, *Fluid Mechanics*, 2nd ed. (Pergamon Press, Oxford, 1987).
- [10] H. Lamb, *Hydrodynamics*, 6th ed. (Cambridge University Press, Cambridge, 1932).